MLH1-mediated recruitment of FAN1 to chromatin for the induction of apoptosis triggered by O^6-methylguanine

Mihoko Rikitake[1,2], Ryosuke Fujikane[1,3], Yuko Obayashi[1,4], Kyoko Oka[2], Masao Ozaki[2], and Masumi Hidaka[1,3,*]

From the [1]Department of Physiological Science and Molecular Biology, Fukuoka Dental College, Fukuoka, 819-0193, Japan, [2]Department of Oral Growth and Development, Fukuoka Dental College, Fukuoka, 819-0193, Japan, [3]Oral Medicine Research Center, Fukuoka Dental College, Fukuoka, 819-0193, Japan, [4]Department of Oral and Maxillofacial Surgery, Fukuoka Dental College, Fukuoka, 819-0193, Japan

A short title: Role of FAN1 in MMR-dependent apoptosis

KEYWORDS: apoptosis, FANCD2 and FANCI-associated nuclease 1 (FAN1), O^6-methylguanine, mismatch repair (MMR), MLH1

To whom correspondence should be addressed; Masumi Hidaka: Department of Physiological Science and Molecular Biology, Fukuoka Dental College, 2-15-1, Tamura, Sawara-ku, Fukuoka, 819-0193, Japan; E-mail: hidaka@college.fdcnet.ac.jp; Tel.: +81-92-801-0411.

Abstract

O^6-Methylguanines (O^6-meG), which are produced in DNA by the action of alkylating agents, are mutagenic and cytotoxic, and induce apoptosis in a mismatch repair (MMR) protein-dependent manner. To understand the molecular mechanism of O^6-meG-induced apoptosis, we performed functional analyses of FANCD2 and FANCI-associated nuclease 1 (FAN1), which was identified as an interacting partner of MLH1. Immunoprecipitation analyses showed that FAN1 interacted with both MLH1 and MSH2 after treatment with *N*-methyl-*N*-nitrosourea (MNU), indicating the formation of a FAN1-MMR complex. In comparison to control cells, *FAN1*-knockdown cells were more resistant to MNU, and the appearances of a sub-G_1 population and caspase-9 activation were suppressed. FAN1 formed nuclear foci in an MLH1-dependent manner after MNU treatment, and some were co-localized with both MLH1 foci and single-stranded DNA (ssDNA) created at damaged sites. Under the same condition, FANCD2 also formed nuclear foci, although it was dispensable for the formation of FAN1 foci and ssDNA. MNU-induced formation of ssDNA was dramatically suppressed in *FAN1*-knockdown cells. We therefore propose that FAN1 is loaded on chromatin through the interaction with MLH1 and produces ssDNA by its exonuclease activity, which contributes to the activation of the DNA damage response followed by the induction of apoptosis triggered by O^6-meG.

1 INTRODUCTION

O^6-Methylguanine (O^6-meG), one of the modified bases produced by the action of Sn1-type alkylating agents, is highly mutagenic because it can pair with thymine as well as cytosine during DNA replication and the resulting O^6-meG/T mismatch in DNA leads to G to A transition mutation after the subsequent round of DNA replication. To protect this outcome, organisms possess a specific repair enzyme, O^6-methylguanine DNA methyltransferase (MGMT), and fix the lesion in a single step reaction (Hayakawa, Koike, & Sekiguchi, 1990; Koike, Maki, Takeya, Hayakawa, & Sekiguchi, 1990). Mouse embryonic stem cells deficient in the methyltransferase gene and some tumor-derived cell lines in which the *MGMT* gene is epigenetically silenced are therefore super-sensitive to alkylating agents, such as *N*-methyl-*N*-nitrosourea (MNU) and *N*-methyl-*N*'-nitro-*N*-nitrosoguanidine (MNNG). (Day et al., 1980; Tominaga, Tsuzuki, Shiraishi, Kawate, & Sekiguchi, 1997). This cytotoxic effect of alkylating agents is caused by the induction of apoptosis, which eliminates cells containing mutation-evoking O^6-meG in a mismatch repair (MMR) protein-dependent manner (Branch, Aquilina, Bignami, & Karran, 1993; Kaina, Ziouta, Ochs, & Coquerelle, 1997; Meikrantz, Bergom, Memisoglu, & Samson, 1998). Mice lacking both *Mgmt* and *Mlh1* genes, the latter which encodes one of the MMR-related proteins, are as resistant to MNU as are wild-type mice in terms of survival, but are much more susceptible to MNU-induced tumorigenesis than wild-type mice (Kawate et al., 1998; Takagi, 2003). In humans, it is well established that MMR deficiency causes hereditary non-polyposis colorectal cancer (HNPCC) (Fishel et al., 1993; Leach et al., 1993; Parsons et al., 1993). These facts indicate that MMR-dependent apoptotic cell death has important roles in preventing a predisposition to tumor development.

The MMR complex, composed of MutSα (MSH2/MSH6 heterodimer) and MutLα (MLH1/PMS2 heterodimer), recognizes O^6-meG/T mismatch produced during the 1st round of

DNA replication (Duckett et al., 1996; Hidaka, Takagi, Takano, & Sekiguchi, 2005; Stojic et al., 2004) and promotes the activation of ATR and CHK1 kinases, which is characterized by the phosphorylation of specific amino acids; however, progression of the cell cycle is not perturbed (Stojic et al., 2004; Yoshioka, Yoshioka, & Hsieh, 2006). Further activation of checkpoint kinases, along with ATM and CHK2, becomes obvious at the next round of the cell cycle, leading to cell cycle arrest at the G_2/M boundary followed by the induction of apoptosis characterized by BAK dimerization, mitochondria outer membrane depolarization and caspase-3/9 activations (Fujikane, Sanada, Sekiguchi, & Hidaka, 2012; Hickman & Samson, 2004; Stojic et al., 2004). Mojas *et al*. reported that futile repair processing of DNA containing O^6-meG/T mismatch by MMR proteins gives rise to single-stranded DNA (ssDNA) gaps, which are converted to double-strand breaks (DSB) during the 2^{nd} round of DNA replication (Mojas, Lopes, & Jiricny, 2007). Such secondary DNA lesions are believed to be responsible for the induction of apoptosis; however, the precise molecular mechanism that processes mismatched DNA and the subsequent DNA damage response (DDR) remains unclear.

In an attempt to reveal the function of the MMR complex in the DNA transaction related to DDR, FAN1/KIAA1018 (FANCD2 and FANCI-associated nuclease 1) was identified as a new interacting partner of an MLH1 by interactome analysis in human cells using tandem affinity purification (Cannavo, Gerrits, Marra, Schlapbach, & Jiricny, 2007). FAN1 is composed of 1017-amino acid residues and possesses an RAD18-lilke ubiquitin-binding zinc finger (UBZ) domain, SAP-type DNA binding domain and virus-type replication repair nuclease (VVR_nuc) domain at its N-terminus, middle and C-terminus, respectively (Kratz et al., 2010; MacKay et al., 2010; Smogorzewska et al., 2010). Depletion of FAN1 from human cells causes hypersensitivity to DNA interstrand crosslinks (ICLs), which block the progression of replication fork, indicating a role of FAN1 in ICL repair. FAN1 is recruited to sub-nuclear foci at the sites of ICLs through the

interaction of its UBZ domain with mono-ubiquitinated FANCD2, which is catalyzed by the E3 ubiquitin ligase FANCL in the Fanconi anemia (FA) core complex (Kratz et al., 2010; MacKay et al., 2010; Meetei et al., 2003; Smogorzewska et al., 2010). FAN1 possesses 5'-flaps endonuclease and 5' to 3' exonuclease activities mediated by its VVR_nuc domain. The functions of these domains are important for the repair of ICLs, since deficiency of either domain confers sensitivity to mitomycin C (MMC) (Kratz et al., 2010; MacKay et al., 2010; Smogorzewska et al., 2010). Although cellular sensitivity to ICLs is representative trait of cells derived from FA patients, FAN1 deficiencies rather result in familial karyomegalic interstitial nephritis (KIN), suggesting that the function of FAN1 is substantially separated from the canonical FA pathway (Lachaud, Moreno, et al., 2016; Lachaud, Slean, et al., 2016; Zhou et al., 2012).

While FAN1 interacts with MLH1, there has been no direct evidence to support the requirement of FAN1 in MMR. Although an *in vitro* reconstitution system of the MMR reaction can be accomplished without FAN1 protein (Constantin, Dzantiev, Kadyrov, & Modrich, 2005), a potential role of Fan1 in MMR *in vivo* has emerged in Exo1-deficient mouse embryonic fibroblasts, in which the Exo1-independent MMR pathway is conducted with the use of other 5' to 3' exonucleases, Fan1, Mre11 and Artemis, in a manner that compensates for the loss of Exo-1 activity (Desai & Gerson, 2014). Furthermore, in humans, nonsynonymous mutations in the *FAN1* gene were found to be responsible for Amsterdam-positive MMR-proficient hereditary non-polyposis colorectal cancers (Segui et al., 2015). These results imply some uncharacterized roles of FAN1 in an MMR pathway.

In the present study, we investigated whether FAN1 is involved in the MMR-dependent apoptotic pathway triggered by O^6-meG in human cells. We demonstrate evidence to support that FAN1 is recruited to damaged chromatin in an MLH1-dependent, but not a FANCD2-dependent, manner and that it contributes to the induction of apoptosis by playing a role in the formation of

ssDNA in the region carrying O^6-meG/T mismatch.

2 RESULTS

2.1 FAN1 associates with the MMR complex in an alkylation-dependent manner

In order to confirm the interaction of FAN1 with MLH1, chromatin-enriched fractions were prepared from MGMT-defective HeLa MR cells after treatment with or without an alkylating agent, MNU, and were subjected to an immunoprecipitation assay using anti-FAN1 or anti-MSH2 antibodies (Figure 1). As shown in Figure 1a, MLH1 was co-precipitated with FAN1, even in the absence of MNU treatment, as previously reported (Cannavo et al., 2007), and the amounts of MLH1 associated with FAN1 were increased after the administration of MNU. MSH2 was also shown to interact with FAN1 in a similar fashion. A reciprocal immunoprecipitation assay using anti-MSH2 antibodies showed MNU-dependent interaction of FAN1 with MSH2 with similar kinetics as MLH1 (Figure 1b). These results suggest that FAN1 interacts with MutLα, even under normal growth conditions and, after MNU treatment, associates with MutSα at the site of DNA carrying O^6-meG/T mismatch.

In Figure 1c, chromatin-enriched fractions were also prepared from cells treated with or without MMC for 12 h to produce ICLs. An immunoprecipitation assay using anti-FAN1 antibody revealed that interactions of FAN1 with MLH1 and MSH2 were not influenced by MMC treatment. As previously reported that FANCD2 is mono-ubiquitinated and recruits FAN1 to damaged chromatin in the FA pathway (Liu, Ghosal, Yuan, Chen, & Huang, 2010; MacKay et al., 2010), a slower migrated band of FANCD2 appeared in the input fraction after MMC treatment and the band, corresponding to mono-ubiquitinated FANCD2, was detected in an immunoprecipitated fraction, confirming the interaction of FAN1 with FANCD2, upon MMC treatment, in a ubiquitination-dependent manner. In contrast, as shown in Figure 1a and b, the

interactions of FANCD2 with FAN1 and MSH2 were hardly detected using chromatin fractions prepared from cells treated with MNU, although FANCD2 was likely to be mono-ubiquitinated, as was evident by the detection of an upper-shifted band in the input fractions after the administration of MNU.

2.2 FAN1 protein is involved in O^6-methylguanine-induced apoptosis

Since FAN1 interacts with not only MLH1 but also MSH2 after MNU treatment, we next examined the possible involvement of FAN1 in an MMR-dependent apoptotic pathway triggered by O^6-meG. *FAN1*-knockdown (*FAN1*-KD) cells were prepared by introducing two independent small interference RNAs (siRNAs), targeting to different FAN1 sequences, to HeLa MR cells. Quantitative real-time PCR analysis revealed that the mRNA levels of the *FAN1* gene in the *FAN1*-KD cells #1 and #2 were reduced to 28.6% and 35.3% of the levels of control cells, respectively (Figure 2a). The obvious suppression of FAN1 protein levels in these knockdown cells was shown by immunoblotting using anti-FAN1 antibodies (Figure 2b). Using these *FAN1*-KD cells, we performed a survival assay with various concentrations of MNU. As shown in Figure 2c, both *FAN1*-KD cells exhibited higher resistance to the killing effect of MNU in comparison to the control cells. This is also the case for U2OS, another human-derived cell line (Figure S1). An *MGMT*-knockout cell line (U2OSΔM) readily underwent cell death after exposure to MNU. In contrast, *FAN1*-knockdown cells #1 also showed increased tolerance to treatment with MNU (Figure S1b).

In order to examine whether acquired resistance of *FAN1*-KD cells to MNU was resulted from the defect of apoptosis induction, the activation of several apoptotic markers in *FAN1*-KD cells was analyzed. As shown in Figure 3a and b, flow cytometry showed that the sub-G_1 population increased after MNU treatment in cells transfected with either type of siRNA; however,

the degree of increase in the *FAN1*-KD cells (12.0%) was significantly suppressed in comparison to the control cells (19.0%). We further analyzed the effect of *FAN1*-KD on the activation of caspase-9 and cleavage of PARP1 in Figure 3c. On immunoblotting, the cleavage of both caspase-9 and PARP1 was clearly observed at 72 h after MNU treatment in siCont-transfected cells. In contrast, in *FAN1*-KD cells, the signals for cleaved-caspase-9 and cleaved-PARP1 were barely detected, even at 72 h. These results clearly indicate that FAN1 is involved in the induction of apoptosis triggered by O^6-meG.

2.3 *FAN1*-knockdown attenuates the activation of the DNA damage response

During the course of the induction of MMR-dependent apoptosis triggered by O^6-mG, the checkpoint kinases (*e.g.*, ATR, CHK1, ATM and CHK2) are known to be activated by phosphorylation at certain amino acid residues of each protein (Fujikane, Komori, Sekiguchi, & Hidaka, 2016; Stojic et al., 2004; Wang & Qin, 2003). To examine the effect of *FAN1*-KD on the activation of the DNA damage response after MNU treatment, the phosphorylation levels of the checkpoint kinases in siRNA-transfected cells were analyzed by immunoblotting (Figure 4). In the siCont-transfected cells, phosphorylation of these proteins was clearly observed at 24 and 48 h after MNU treatment, as expected. In contrast, the phosphorylation levels of these proteins were decreased at both 24 and 48 h after MNU treatment. These results suggest that the association of FAN1 with the MMR complex promotes proper activation of the DNA damage response triggered by O^6-meG.

2.4 FAN1 is loaded on damaged chromatin in an MLH1-dependent manner

When cells are treated with MNU, MLH1 is loaded on chromatin to recognize O^6-meG /T mismatch coupled with DNA replication. Since FAN1 has been found to interact with MLH1, it

might be possible that FAN1 is also loaded on chromatin after MNU treatment (Cannavo et al., 2007). To examine this possibility, cells were treated with MNU, followed by cultivation for 0, 24 and 48 h, and cytoplasmic and chromatin-bound fractions were prepared. Immunoblotting revealed that, in MLH1-proficient HeLa MR cells, chromatin-bound MLH1 increased after MNU treatment, as expected, and that the chromatin-bound FAN1 also increased in a similar fashion to MLH1 (Figure 5a). In *MLH1*-konckout cells, on the other hand, this increase of chromatin-bound FAN1 was not observed. These results indicate that after MNU treatment, FAN1 is loaded on chromatin in an MLH1-dependent manner.

FANCD2 is another candidate, which could recruit FAN1 to damaged chromatin, as is evident when cells are treated with MMC. To examine whether this is also the case in cells treated with MNU, chromatin extracts were prepared from siFANCD2-transfected cells and subjected to immunoblotting using specific antibodies. As shown in Figure 5b, the amounts of chromatin-bound FAN1 and MLH1, in *FANCD2*-KD cells, increased after MNU treatment and were comparable to those in the control cells, indicating that FANCD2 is dispensable for chromatin-loading of FAN1 after MNU treatment. It should be noted that, under this *FANCD2*-knockdown condition, *FANCD2*-KD cells were more sensitive to MMC than the control cells, whereas their degree of sensitivity to MNU was similar to that of control cells (Figure S2).

2.5 FAN1 forms nuclear foci and is co-localized with MLH1 in MNU-treated cells

In order to examine the sub-localization of FAN1 in cells, we performed an indirect immunofluorescent analysis using a laser confocal microscope. In order to visualize FAN1 signals specifically and clearly in the analyses, we constructed HeLa MR cells that stably expressed exogenous FAN1 (MR+pEB-FAN1), which produced approximately 1.5 times as much total FAN1 as the endogenous FAN1 protein. The sensitivity of the cells to MNU was similar to that

of the parental HeLa MR cells (Figure S3). As shown in Figure 6a, in siCont-transfected cells, FAN1 signals were hardly observed without MNU treatment, whereas FAN1 formed nuclear foci at 48 h after MNU treatment. MLH1 also formed nuclear foci after MNU treatment, some of which appeared to be co-localized with FAN1 and some of which were adjacent to FAN1. Statistical analyses revealed that the number of foci merged between FAN1 and MLH1 was significantly correlated with the number of FAN1 foci ($r = 0.64$, $p = 9.57 \times 10^{-5}$) or MLH1 foci ($r = 0.57$, $p = 2.12 \times 10^{-3}$), respectively (Figure 6b). Approximately 30% of FAN1 was co-localized with MLH1, whereas approximately 45% of MLH1 foci was co-localized with FAN1 foci. It is noteworthy that approximately 65% of FAN1 signals were co-localized with BrdU foci, which represent ssDNA regions, formed upon the production of O^6-meG/T mismatch in DNA. The detection of ssDNA was achieved because the BrdU incorporated in DNA is detectable by anti-BrdU antibody without denaturation of DNA only when BrdU is exposed in ssDNA (Couch et al., 2013). It was also demonstrated that approximately 20% of FAN1 foci were co-localized with both MLH1 and BrdU. In siMLH1-transfected cells, on the other hand, the formation of nuclear foci of both FAN1 and BrdU after MNU treatment was diminished (Figure 6a). The results further support the hypothesis that FAN1 is recruited to damaged chromatin through interaction with MLH1.

We further examined the effect of *FANCD2*-KD on the focus-formation of FAN1 and BrdU (Figure 6c). In siCont-transfected cells, after exposure to MNU, FANCD2 also formed nuclear foci and some of them were co-localized with FAN1 and/or BrdU. The introduction of siRNA specific for the *FANCD2* gene severely suppressed the signal of FANCD2. Nevertheless, FAN1 formed nuclear foci and was co-localized with BrdU. In addition, the focus formation of MLH1 and co-localization of FAN1 with MLH1 after MNU treatment were unaffected by *FANCD2*-KD (Figure S4). These results suggest that FANCD2 is not relevant to the focus-

formation of FAN1 and the production of ssDNA in response to MNU treatment.

2.6 FAN1 is involved in the formation of ssDNA after MNU treatment.

Since FAN1 possesses 5' to 3' exonuclease activity (Kratz et al., 2010; Liu et al., 2010; MacKay et al., 2010; Smogorzewska et al., 2010), it might be possible that FAN1 contributes to the formation of ssDNA by processing the site containing DNA mismatch. To investigate this possibility, HeLa MR cells were transfected with siFAN1, then treated with MNU or left untreated and subjected to immunofluorescence analyses (Figure 7a). Consistent with the results obtained in Figure 6, the number of BrdU foci in the control cells after MNU treatment (4.64 foci/nucleus in average) was 11 times that under untreated condition (0.40 foci/nucleus) (Figure 7b). In *FAN1*-KD cells, the number of BrdU foci decreased significantly to 2.77 foci/nucleus, even after exposure to MNU. In contrast, the number of MLH1 foci formed in the control cells after MNU treatment was unaffected by the suppression of FAN1 expression (3.28 foci/nucleus in control cells vs. 4.30 foci/nucleus in *FAN1*-KD cells) (Figure S5). This is also the case for another human-derived cell line (U2OSΔM). The number of BrdU foci in *FAN1*-KD cells decreased dramatically, even after exposure to MNU, in comparison to those in the control cells (Figure S6). These results strongly suggest that FAN1 loaded on chromatin plays a role in the processing of O^6-meG/T mismatch-containing DNA, possible through its nuclease activity, and in the production of ssDNA in the pathway of MMR-dependent apoptosis.

3 DISCUSSION

FAN1 was originally identified as a novel MLH1-interacting protein by an interactome analysis using TAP-tagged MLH1 expressed exogenously in human cells (Cannavo et al., 2007). However, the biological roles of the interaction between FAN1 and MLH1 are currently unknown. In this

report, we demonstrate that FAN1 plays a role in the induction of apoptosis through the interaction with the MMR complex, which consists of MutSα and MutLα, at the site of base-mismatch raised by treatment with an alkylating agent, MNU. Our results showed that the knockdown of the *FAN1* gene in HeLa MR cells conferred tolerance to the killing effect of MNU. In *FAN1*-KD cells, the MNU-induced production of sub-G_1 population and cleavage of both caspase-9 and PARP1 were suppressed in comparison to control cells. In addition, *FAN1*-KD attenuated the phosphorylation levels of ATR, CHK1, ATM and CHK2 kinases after MNU treatment, indicating that FAN1 is required for full activation of DDR to arrest cell cycle at G_2/M boundary prior to the induction of apoptosis. It was reported, based on the biochemical characterization of recombinant human FAN1 protein, that the protein possesses 5'-flap endonuclease and 5' to 3' exonuclease activities mediated by its conserved VRR_nuc domain (Liu et al., 2010; MacKay et al., 2010; Smogorzewska et al., 2010). In accordance with these activities, we showed that the formation of ssDNA induced after MNU treatment was severely suppressed in *FAN1*-KD cells. Taken together with these results, we herein propose a possible model of an MNU-induced apoptosis pathway in which FAN1 is recruited to MutSα-bound chromatin by MutLα, through interaction with MLH1, and excises mismatch-containing DNA by its exonuclease activity. The resulting ssDNA formed would be coated with RPA and would activate ATR/CHK1-axis signaling followed by the induction of apoptosis (Figure 8).

An argument is raised as to why the repression of DDR activation and the induction of apoptosis is limited in *FAN1*-KD cells while the expression of FAN1 is effectively suppressed (see Figure 1). This could be explained by the existence of backup nucleases that compensate for the FAN1 function in the MMR-dependent apoptosis pathway. It is well known that EXO1 is a major 5' to 3' exonuclease that plays a role in the MMR reaction. In addition, other 5' to 3' exonucleases (*e.g.*, FAN1, MRE11 and ARTEMIS [SNM1C]), might also work in the excision of

mismatched DNA, since the gene knockdown of each nuclease in *Exo1*-deficient MEF rendered the cells to more resistant to temozolomide, another alkylating agent that produces O^6-meG in DNA (Desai & Gerson, 2014). Similarly, *FAN1/EXO1/FEN1*-triple knockdown cells derived from HeLa MR cells showed higher degree of resistance to the killing effect of MNU in comparison to *FAN1*-single knockdown cells (Rikitake et al., unpublished data). Thus, it is highly possible that multiple nucleases are redundantly involved in the MMR-dependent apoptosis by compensating each other in order to maintain genome homeostasis.

We unexpectedly found that FANCD2 was modified (highly possibly by mono-ubiquitination) and formed nuclear foci after treatment with MNU. It was shown that the modification and chromatin-loading of FANCD2 were dependent on MLH1 (see Figure 5a), although these were dispensable for the recruitment of FAN1 to damaged chromatin. This finding suggests that a certain type of DNA replication stress might be generated once the MMR complex recognizes O^6-meG/T mismatch in DNA and that FANCD2 could have an uncharacterized role in responding to the stress.

Although it has not been determined whether the UBZ domain of FAN1 is required for its focus formation in the nucleus following MNU treatment, the present study revealed an important role of FAN1 in the O^6-meG-induced apoptosis in which FAN1 is recruited to chromatin in an MLH1-dependent manner. FAN1 is known to be involved in the recovery from DNA replication stress caused by ICL through the interaction between its UBZ domain and ubiquitinated FANCD2. It has also been reported that the UBZ domain of FAN1 is able to bind to mono-ubiquitinated PCNA at K164, which is a prerequisite reaction for recovery from the stress caused by G4 DNAs (Porro et al., 2017). Furthermore, several reports have shown that exogenously expressed FAN1 variants carrying a mutation in their UBZ domain were able to form nuclear foci in response to replication stress, and complement the sensitivity to MMC in FAN1-

deficient cells (Chaudhury, Stroik, & Sobeck, 2014; Lachaud, Moreno, et al., 2016; Porro et al., 2017). Recently, nonsynonymous mutations in the *FAN1* gene were found to be associated with the MMR-proficient microsatellite-stable colorectal cancers (Segui et al., 2015) and a novel hereditary pancreatic adenocarcinoma (Smith et al., 2016). Moreover, FAN1 was shown to be involved in prevention of the expansion of triplet repeat sequences that causes Huntington disease and Fragile X syndrome (Goold et al., 2018; Zhao & Usdin, 2018). The identification of *FAN1* mutations in such diseases suggests that *FAN1*-deficiency might impair the function of MMR, leading to tumors relevant to MMR-deficiency. Further functional studies on the association between FAN1 and MMR should be performed to understand the molecular mechanisms underlying these diseases.

4 EXPERIMENTAL PROCEDERES

4.1 Cell lines and culture

HeLa S3-derived HeLa MR cells defective in the MGMT function (Laboratory stock), HeLa MR-derived *MLH1*-knockout cells (Takeishi et al., 2019) and U2OS-derived *MGMT*-knockout cells (Takeishi et al., 2019) were cultivated in Dulbecco's Modified Eagle Medium (D-MEM, FUJIFILM Wako Pure Chemicals, Osaka, Japan) supplemented with 10% fetal bovine serum and penicillin/streptomycin (FUJIFILM Wako Pure Chemicals) in 5% CO_2 at 37°C.

4.2 Construction of a cell line overexpressing FAN1

The cDNAs were synthesized, using total RNAs prepared from HeLa MR cells, by Prime script 1st strand cDNA synthesis kit (Takara Bio., Shiga, Japan). FAN1 cDNA was amplified by PCR using PrimeStar GXL polymerase (Takara Bio.) with the following primers 5'-AAGGGGTACCATGATGTCAGAAGGGAAACCTCCTGAC-3' and 5'-

GCTTATCGATTTAGCTAAGGCTTTGGCTCTTAGCTCCAAC-3'. The PCR fragment was cloned into pEBMulti-Hyg vector (FUJIFILM-Wako Pure Chemicals) at the KpnI/ClaI site, and the nucleotide sequence was confirmed by DNA sequencing. The resulting plasmid, designated as pEB-FAN1, was introduced into HeLa MR cells by lipofectamine 2000 (Thermo Fisher Scientific, MA, USA) according to the manufacturer's instruction. The transfected cells were cultivated in medium containing 0.3 mg/ml Hygromycin B. The overexpression of FAN1 was confirmed by immunoblotting.

4.3 Gene knockdown with siRNA

Silencer Select siRNAs targeting the *FAN1* gene (#1; 5'-GCUGGACAGUCAGUACGAATT-3' and #2; 5'-GUAAGGCUCUUUCAACGUATT-3') or *FANCD2* gene (5'-GCACCGUAUUCAAGUACAATT-3') and Stealth RNAi for the *MLH1* gene (5'-UGCACAUUAACAUCCACAUUCUGGG-3') were purchased from Thermo Fisher Scientific. HeLa MR or U2OSΔM cells were transfected with appropriate siRNA using Lipofectamine RNAiMax (Thermo Fisher Scientific) according to manufacturer's instruction manual. The transfected cells were cultured for two days, then were used for the assays. At three days after transfection, the knockdown efficiency was verified by immunoblotting and quantitative PCR.

4.4 Quantitative PCR

Total RNAs were prepared using an RNeasy mini kit (Qiagen, Hilden, Germany) and cDNAs were synthesized using a Prime script 1st strand cDNA synthesis kit (Takara Bio.), according to the instruction manual. Quantitative PCR was performed using a CFX96 Touch Real-time detection system with SsoAdvanced Universal SYBR Green Supermix (Bio-Rad Laboratories, CA, USA) and the following primers: FAN1qPCR-F; 5'-

GGGCAAGAATAAGCCTGGAATTGGTGC-3' and FAN1qPCR-R; 5'-AAGCGGCGTCTTCATCTTCCATTGAGTC-3', or FANCD2qPCR-F; 5'-CCCAAGAGAGAGCCAACCTG-3' and FANCD2qPCR-R; 5'-GGTATGCCCAACCCATTCCA-3'. The quantitative PCR data were analyzed using the CFX Maestro software program (Bio-Rad Laboratories).

4.5 Survival assay

Five hundred cells were placed in 100-mm dishes one day before MNU treatment, and treated with various concentrations of MNU or MMC for 1 h in serum-free D-MEM with 20 mM Hepes-KOH (pH6.0) or in serum-free D-MEM, respectively, followed by cultivation in serum-supplemented D-MEM for 10 days. Surviving colonies were stained with 0.1% crystal violet and counted, and survival rates were calculated.

4.6 Immunoblotting

Protein samples prepared from cells were subjected to SDS-PAGE and then electrotransferred to a PVDF membrane (Bio-Rad Laboratories). The PVDF membrane was immersed with the Can Get Signal PVDF blocking Reagent (TOYOBO, Osaka, Japan) and incubated with the primary antibody diluted in Can Get Signal Immunostain Solution A (TOYOBO). After washing with PBS containing 0.1% Tween 20 (PBS-T), the membrane was blotted with HRP-conjugated secondary antibody (GE Healthcare) in Can Get Signal Immnostain Solution B (TOYOBO) for 1 h and visualized with a chemiluminescent agent (ImmunoStar LD; FUJIFILM-Wako Pure Chemicals) by an LAS-4010 (GE Healthcare Life Sciences, Amersham, UK).

4.7 Antibodies

Anti-FAN1 (#17600-AP-1), anti-β-actin (#A5316) and anti-phospho-ATR-T1989 (#GTX128145) were purchased from Proteintech, Merck and GeneTex, respectively. Anti-BrdU (#ab6326) and Alexa647-anti-mouse IgG (#ab150107) were purchased from Abcam, Cambridge, UK. Anti-caspase9 (#9502), anti-CHK2 (#6334), anti-FANCD2 (#16323), anti-phospho-ATM-S1981 (#13050), anti-phospho-CHK1-S317 (#12302) and anti-phospho-CHK2-T68 (#2661) were obtained from Cell Signaling Tech., MA, USA. Anti-MLH1 (#554073), anti-MSH6 (#610918) and anti-PMS2 (#556415) were purchased from BD Biosciences, NJ, USA. Alexa488-anti-mouse IgG (#A11029), Alexa568-anti-rat IgG (#A11077), Alexa488-anti-rabbit IgG (#A11034) and anti-MSH2 (#337900) were purchased from Thermo Fisher Scientific. Anti-ATR (#sc1887), anti-CHK1 (#sc8408), anti-FANCD2 (#sc20022) and anti-PARP1 (#sc8007) were purchased from Santa Cruz Biotech, TX, USA.

4.8 Flow cytometry

HeLa MR cells transfected with siCont or siFAN1 with or without treatment with MNU were incubated in a complete medium. The cells were harvested by the treatment with trypsin-EDTA and collected by centrifugation. The resultant cells were suspended with PBS containing 0.1% Triton X-100, 10 μg/ml of RNase A, and 0.25% propidium iodide. Samples were analyzed using a FACS Calibur flow cytometer (BD Biosciences) until the gated events reached 10,000.

4.9 Cell fractionation

To prepare the chromatin fraction, cells were washed with ice cold PBS and then suspended in mCSK buffer (10 mM PIPES-NaOH, pH 6.8, 100 mM NaCl, 300 mM sucrose, 1 mM EGTA, 1 mM $MgCl_2$, and 0.1% Triton X-100). The cells were incubated for 10 min on ice, and nuclei were collected by low-speed centrifugation. The supernatant was further clarified by high-speed

centrifugation and used as the cytoplasmic fraction. Nuclei were washed once in mCSK buffer and then lysed in SDS-sample buffer, followed by brief sonication and boiling.

4.10 Immunoprecipitation analysis

The cells with or without treatment with 1 mM MNU or 10 μM Mytomycin C for 1 h in serum-free D-MEM were further cultivated in complete medium. When harvesting, the cells were treated on a dish with a hypotonic buffer (20 mM Hepes-KOH, pH7.4, 5 mM KCl, 1.5 mM $MgCl_2$, 0.1 mM Dithiothreitol and 100 μg/ml Digitonin) for 10 min and then washed once with PBS. The cells were fixed with 1% formaldehyde for 10 min at RT, followed by quenching by adding 1 M Tris-HCl (pH 8.0), and then harvested and collected by centrifugation. The cell pellet was suspended in RIPA buffer (10 mM Tris-HCl [pH 8.0], 150 mM NaCl, 1% NP40, 0.5% deoxycholate, and 0.1% SDS) and sonicated, followed by centrifugation to obtain supernatant as chromatin-enriched fraction. The supernatant was mixed with anti-FAN1 or anti-MSH2 antibody for 1 h at 4°C, and further incubated with Protein G-conjugated Sepharose beads (GE Healthcare Life Sciences). After washing the beads with RIPA buffer five-times, the proteins bound to the beads were eluted and boiled with SDS-sample buffer containing 1% β-mercaptoethanol for 10 min, and then subjected to SDS-PAGE and immunoblotting with appropriate antibodies.

4.11 Immunofluorescence analysis

Cells grown in medium containing 20 μM bromodeoxyuridine in a film-bottom dish (Matsunami Glass Ind., Osaka, Japan) were treated with 25 μM MNU and further cultivated for 48 h. The cells were treated with mCSK buffer (10 mM PIPES-NaOH, pH 6.8, 100 mM NaCl, 300 mM sucrose, 1 mM EGTA, 1 mM $MgCl_2$, and 0.1% Triton X-100) for 5 min at 4°C and washed twice with ice-cold PBS. After fixation of the cells with 4% paraformaldehyde for 15 min, the cells were

incubated with a blocking solution (PBS containing 0.1% Tween 20 and 2% BSA) and mixed with appropriate antibodies overnight, followed by further incubation with appropriate combination of Alexa Fluoro488/568/647-conjugated antibodies. The samples were observed under a confocal laser scanning microscope, LSM710 (Carl Zeiss, Oberkochen, Germany). The number of foci were counted using the Image J software program (https://imagej.nih.gov/ij/) with the speckle inspector plug-in in the BioVoxxel tool box (https://imagej.net/BioVoxxel_Toolbox).

ACKNOWLEDGMENTS

The authors thank Dr Y. Takeishi at Fukuoka Dental College for helpful discussion. This work was supported by The Private University Research Branding Project and JSPS KAKENHI Grant-in-Aid for Young Scientist (B) Grant Number 26830085 (to R.F.), and JSPS KAKENHI Grant-in-Aid for Scientific research (A) Grant Number 25241012 (to M.H.).

ORCID

Masumi Hidaka https://orcid.org/0000-0002-1901-2955

REFERENCES

Branch, P., Aquilina, G., Bignami, M., & Karran, P. (1993). Defective mismatch binding and a mutator phenotype in cells tolerant to DNA damage. *Nature, 362*(6421), 652-654. doi: 10.1038/362652a0

Cannavo, E., Gerrits, B., Marra, G., Schlapbach, R., & Jiricny, J. (2007). Characterization of the interactome of the human MutL homologues MLH1, PMS1, and PMS2. *J Biol Chem, 282*(5), 2976-2986. doi: 10.1074/jbc.M609989200

Chaudhury, I., Stroik, D. R., & Sobeck, A. (2014). FANCD2-controlled chromatin access of the

Fanconi-associated nuclease FAN1 is crucial for the recovery of stalled replication forks. *Mol Cell Biol, 34*(21), 3939-3954. doi: 10.1128/MCB.00457-14

Constantin, N., Dzantiev, L., Kadyrov, F. A., & Modrich, P. (2005). Human mismatch repair: reconstitution of a nick-directed bidirectional reaction. *J Biol Chem, 280*(48), 39752-39761. doi: 10.1074/jbc.M509701200

Couch, F. B., Bansbach, C. E., Driscoll, R., Luzwick, J. W., Glick, G. G., Betous, R., . . . Cortez, D. (2013). ATR phosphorylates SMARCAL1 to prevent replication fork collapse. *Genes Dev, 27*(14), 1610-1623. doi: 10.1101/gad.214080.113

Day, R. S., 3rd, Ziolkowski, C. H., Scudiero, D. A., Meyer, S. A., Lubiniecki, A. S., Girardi, A. J., . . . Bynum, G. D. (1980). Defective repair of alkylated DNA by human tumour and SV40-transformed human cell strains. *Nature, 288*(5792), 724-727. doi: 10.1038/288724a0

Desai, A., & Gerson, S. (2014). Exo1 independent DNA mismatch repair involves multiple compensatory nucleases. *DNA Repair (Amst), 21*, 55-64. doi: 10.1016/j.dnarep.2014.06.005

Duckett, D. R., Drummond, J. T., Murchie, A. I., Reardon, J. T., Sancar, A., Lilley, D. M., & Modrich, P. (1996). Human MutSalpha recognizes damaged DNA base pairs containing O6-methylguanine, O4-methylthymine, or the cisplatin-d(GpG) adduct. *Proc Natl Acad Sci U S A, 93*(13), 6443-6447. doi: 10.1073/pnas.93.13.6443

Fishel, R., Lescoe, M., Rao, M., Copeland, N., Jenkins, N., Garber, J., . . . Kolodner, R. (1993). The human mutator gene homolog MSH2 and its association with hereditary nonpolyposis colon cancer. *Cell, 75*, 1027-1038.

Fujikane, R., Komori, K., Sekiguchi, M., & Hidaka, M. (2016). Function of high-mobility group A proteins in the DNA damage signaling for the induction of apoptosis. *Sci Rep, 6*, 31714.

doi: 10.1038/srep31714

Fujikane, R., Sanada, M., Sekiguchi, M., & Hidaka, M. (2012). The identification of a novel gene, MAPO2, that is involved in the induction of apoptosis triggered by O(6)-methylguanine. *PLoS One, 7*(9), e44817. doi: 10.1371/journal.pone.0044817

Goold, R., Flower, M., Moss, D. H., Medway, C., Wood-Kaczmar, A., Andre, R., . . . Tabrizi, S. J. (2018). FAN1 modifies Huntington's disease progression by stabilising the expanded HTT CAG repeat. *Hum Mol Genet*. doi: 10.1093/hmg/ddy375

Hayakawa, H., Koike, G., & Sekiguchi, M. (1990). Expression and cloning of complementary DNA for a human enzyme that repairs O6-methylguanine in DNA. *J Mol Biol, 213*, 739-747.

Hickman, M., & Samson, L. (2004). Apoptotic signaling in response to a single type of DNA lesion, O(6)-methylguanine. *Mol Cell, 14*, 105-116.

Hidaka, M., Takagi, Y., Takano, T. Y., & Sekiguchi, M. (2005). PCNA-MutSalpha-mediated binding of MutLalpha to replicative DNA with mismatched bases to induce apoptosis in human cells. *Nucleic Acids Res, 33*(17), 5703-5712. doi: 10.1093/nar/gki878

Kaina, B., Ziouta, A., Ochs, K., & Coquerelle, T. (1997). Chromosomal instability, reproductive cell death and apoptosis induced by O6-methylguanine in Mex-, Mex+ and methylation-tolerant mismatch repair compromised cells: facts and models. *Mutat Res, 381*(2), 227-241. doi: 10.1016/s0027-5107(97)00187-5

Kawate, H., Sakumi, K., Tsuzuki, T., Nakatsuru, Y., Ishikawa, T., Takahashi, S., . . . Sekiguchi, M. (1998). Separation of killing and tumorigenic effects of an alkylating agent in mice defective in two of the DNA repair genes. *Proc Natl Acad Sci U S A, 95*, 5116-5120.

Koike, G., Maki, H., Takeya, H., Hayakawa, H., & Sekiguchi, M. (1990). Purification, structure, and biochemical properties of human O6-methylguanine-DNA methyltransferase. *J Biol*

Chem, 265(25), 14754-14762.

Kratz, K., Schopf, B., Kaden, S., Sendoel, A., Eberhard, R., Lademann, C., . . . Jiricny, J. (2010). Deficiency of FANCD2-associated nuclease KIAA1018/FAN1 sensitizes cells to interstrand crosslinking agents. *Cell, 142*(1), 77-88. doi: 10.1016/j.cell.2010.06.022

Lachaud, C., Moreno, A., Marchesi, F., Toth, R., Blow, J. J., & Rouse, J. (2016). Ubiquitinated Fancd2 recruits Fan1 to stalled replication forks to prevent genome instability. *Science, 351*(6275), 846-849. doi: 10.1126/science.aad5634

Lachaud, C., Slean, M., Marchesi, F., Lock, C., Odell, E., Castor, D., . . . Rouse, J. (2016). Karyomegalic interstitial nephritis and DNA damage-induced polyploidy in Fan1 nuclease-defective knock-in mice. *Genes Dev, 30*(6), 639-644. doi: 10.1101/gad.276287.115

Leach, F. S., Nicolaides, N. C., Papadopoulos, N., Liu, B., Jen, J., Parsons, R., . . . et al. (1993). Mutations of a mutS homolog in hereditary nonpolyposis colorectal cancer. *Cell, 75*(6), 1215-1225. doi: 10.1016/0092-8674(93)90330-s

Liu, T., Ghosal, G., Yuan, J., Chen, J., & Huang, J. (2010). FAN1 acts with FANCI-FANCD2 to promote DNA interstrand cross-link repair. *Science, 329*(5992), 693-696. doi: 10.1126/science.1192656

MacKay, C., Declais, A. C., Lundin, C., Agostinho, A., Deans, A. J., MacArtney, T. J., . . . Rouse, J. (2010). Identification of KIAA1018/FAN1, a DNA repair nuclease recruited to DNA damage by monoubiquitinated FANCD2. *Cell, 142*(1), 65-76. doi: 10.1016/j.cell.2010.06.021

Meetei, A. R., de Winter, J. P., Medhurst, A. L., Wallisch, M., Waisfisz, Q., van de Vrugt, H. J., . . . Wang, W. (2003). A novel ubiquitin ligase is deficient in Fanconi anemia. *Nat Genet, 35*(2), 165-170. doi: 10.1038/ng1241

Meikrantz, W., Bergom, M. A., Memisoglu, A., & Samson, L. (1998). O6-alkylguanine DNA lesions trigger apoptosis. *Carcinogenesis, 19*(2), 369-372. doi: 10.1093/carcin/19.2.369

Mojas, N., Lopes, M., & Jiricny, J. (2007). Mismatch repair-dependent processing of methylation damage gives rise to persistent single-stranded gaps in newly replicated DNA. *Genes Dev, 21*(24), 3342-3355. doi: 10.1101/gad.455407

Parsons, R., Li, G. M., Longley, M. J., Fang, W. H., Papadopoulos, N., Jen, J., . . . Modrich, P. (1993). Hypermutability and mismatch repair deficiency in RER+ tumor cells. *Cell, 75*(6), 1227-1236. doi: 10.1016/0092-8674(93)90331-j

Porro, A., Berti, M., Pizzolato, J., Bologna, S., Kaden, S., Saxer, A., . . . Jiricny, J. (2017). FAN1 interaction with ubiquitylated PCNA alleviates replication stress and preserves genomic integrity independently of BRCA2. *Nat Commun, 8*(1), 1073. doi: 10.1038/s41467-017-01074-6

Segui, N., Mina, L. B., Lazaro, C., Sanz-Pamplona, R., Pons, T., Navarro, M., . . . Valle, L. (2015). Germline Mutations in FAN1 Cause Hereditary Colorectal Cancer by Impairing DNA Repair. *Gastroenterology, 149*(3), 563-566. doi: 10.1053/j.gastro.2015.05.056

Smith, A. L., Alirezaie, N., Connor, A., Chan-Seng-Yue, M., Grant, R., Selander, I., . . . Zogopoulos, G. (2016). Candidate DNA repair susceptibility genes identified by exome sequencing in high-risk pancreatic cancer. *Cancer Lett, 370*(2), 302-312. doi: 10.1016/j.canlet.2015.10.030

Smogorzewska, A., Desetty, R., Saito, T. T., Schlabach, M., Lach, F. P., Sowa, M. E., . . . Elledge, S. J. (2010). A genetic screen identifies FAN1, a Fanconi anemia-associated nuclease necessary for DNA interstrand crosslink repair. *Mol Cell, 39*(1), 36-47. doi: 10.1016/j.molcel.2010.06.023

Stojic, L., Mojas, N., Cejka, P., Di Pietro, M., Ferrari, S., Marra, G., & Jiricny, J. (2004). Mismatch

repair-dependent G2 checkpoint induced by low doses of SN1 type methylating agents requires the ATR kinase. *Genes Dev, 18*(11), 1331-1344. doi: 10.1101/gad.294404

Takagi, Y. (2003). Roles of MGMT and MLH1 proteins in alkylation-induced apoptosis and mutagenesis. *DNA Repair, 2*(10), 1135-1146. doi: 10.1016/s1568-7864(03)00134-4

Takeishi, Y., Fujikane, R., Rikitake, M., Obayashi, Y., Sekiguchi, M., & Hidaka, M. (2019). SMARCAD1-mediated recruitment of the DNA mismatch repair protein MutLalpha to MutSalpha on damaged chromatin induces apoptosis in human cells. *J Biol Chem*. doi: 10.1074/jbc.RA119.008854

Tominaga, Y., Tsuzuki, T., Shiraishi, A., Kawate, H., & Sekiguchi, M. (1997). Alkylation-induced apoptosis of embryonic stem cells in which the gene for DNA-repair, methyltransferase, had been disrupted by gene targeting. *Carcinogenesis, 18*, 889-896.

Wang, Y., & Qin, J. (2003). MSH2 and ATR form a signaling module and regulate two branches of the damage response to DNA methylation. *Proc Natl Acad Sci U S A, 100*(26), 15387-15392. doi: 10.1073/pnas.2536810100

Yoshioka, K., Yoshioka, Y., & Hsieh, P. (2006). ATR kinase activation mediated by MutSalpha and MutLalpha in response to cytotoxic O6-methylguanine adducts. *Mol Cell, 22*(4), 501-510. doi: 10.1016/j.molcel.2006.04.023

Zhao, X. N., & Usdin, K. (2018). FAN1 protects against repeat expansions in a Fragile X mouse model. *DNA Repair (Amst), 69*, 1-5. doi: 10.1016/j.dnarep.2018.07.001

Zhou, W., Otto, E. A., Cluckey, A., Airik, R., Hurd, T. W., Chaki, M., . . . Hildebrandt, F. (2012). FAN1 mutations cause karyomegalic interstitial nephritis, linking chronic kidney failure to defective DNA damage repair. *Nat Genet, 44*(8), 910-915. doi: 10.1038/ng.2347

FIGURES LEGENDS

FIGURE 1 FAN1 interacts with the mismatch repair complex after MNU treatment. (a) HeLa MR cells were treated with 1 mM MNU and chromatin-enriched fraction (input) were prepared at the indicated time points. Anti-FAN1 antibody-conjugated beads were incubated with the fraction and the precipitants with beads were subjected to SDS-PAGE, followed by immunoblotting using the indicated antibodies. (b) The immunoprecipitation assay performed with an anti-MSH2 antibody was analyzed as described in (a). (c) HeLa MR cells were treated with 1 μM mitomycin C (MMC) and chromatin-enriched fraction (input) were prepared at 12 h after the treatment. The immunoprecipitation analysis using anti-FAN1 antibody was performed as described in (a).

FIGURE 2 The sensitivity of *FAN1*-knockdown cells to the treatment with MNU. Two independent siRNAs targeting to different sequences of the *FAN1* gene were transfected into HeLa MR cells. (a) The mRNA levels of *FAN1* were analyzed by quantitative PCR at two days after siRNA-transfection. The mean values of the relative *FAN1*-expression levels in comparison to control were obtained from three independent experiments and are shown with the S.E. (b) The FAN1 protein levels at three days after siRNA-transfection were analyzed by immunoblotting. β-actin was the loading control. (c) The survival fraction of siRNA-transfected cells after MNU treatment. The cells were treated with various concentrations of MNU and the number of colonies formed at 10 days after the treatment was counted. The mean values of survival fraction obtained from three independent experiments is shown with the S.E. * $p < 0.05$ (Student's *t*-test).

FIGURE 3 Suppression of apoptotic events in *FAN1*-knockdown cells treated with MNU. (a) siFAN1- or siCont-transfected cells were treated with 25 μM MNU or left untreated, and then

cultivated for 72 h. The cells were collected and subjected to flow cytometry. Representative profiles of these cells are shown. (b) The mean values of the sub-G_1 population obtained from three independent experiments and S.E. are shown * $p < 0.05$ (Student's *t*-test). (c) siFAN1- or siCont- transfected cells were exposed to 25 μM MNU and incubated for 0, 48 and 72 h. Whole cells extracts were prepared and subjected to immunoblotting using specific antibodies recognizing both uncleaved and cleaved forms of the protein. β-actin was the loading control.

FIGURE 4 Suppression of DNA damage signaling in *FAN1*-knockdown cells after MNU treatment. HeLa MR cells transfected with siFAN1 or siCont were treated with 25 μM MNU and then cultivated for 0, 24 and 48 h. Whole cell extracts were prepared and subjected to SDS-PAGE, followed by immunoblotting using the indicated antibodies. β-actin was the loading control.

FIGURE 5 Chromatin loading of FAN1 after MNU treatment is dependent on MLH1, but not FANCD2. (a) HeLa MR and *MLH1*-knockout (ΔMLH1) cells were treated with 25 μM MNU and then cultivated for 0, 24 and 48 h. The cells were fractionated into cytoplasmic (Cyto) and chromatin (Chr) fractions and then subjected to SDS-PAGE followed by immunoblotting using the indicated antibodies. MEK2 and HP1α/β are fractionation markers for cytoplasmic and chromatin fractions, respectively. (b) HeLa MR cells transfected with siFANCD2 or siCont were treated with 25 μM MNU. Biochemical fractionation and immunoblotting analysis were performed as described in (a).

FIGURE 6 FAN1 forms nuclear foci in MLH1-dependent, but not FANCD2-dependent manner and is co-localized with ssDNA. (a) The cells overexpressing FAN1 were transfected with siMLH1 or siCont. Two days later, they were treated with 25 μM MNU or left untreated, and

incubated for 48 h. The cells were permeabilized with 0.1% Triton X-100 and fixed with 4% paraformaldehyde followed by immunofluorescence analyses using the indicated antibodies. The nuclei were stained with DAPI. Scale bar represents 10 μm. (b) A scatterplot demonstrating the numbers of FAN1 foci or MLH1 foci vs. the numbers of merged foci (*n*=26). The correlation coefficient (r) and its significance (p) were calculated and are indicated in the plot. (c) The cells overexpressing FAN1 were transfected with siFANCD2 or siCont. Two days later, they were treated with 25 μM MNU or left untreated, and incubated for 48 h. Immunofluorescence analyses were performed as described in (a).

FIGURE 7 A role of FAN1 in the formation of ssDNA after MNU treatment. (a) HeLa MR cells transfected with siFAN1 or siCont were treated with 25 μM MNU or left untreated, and incubated for 48 h. Immunofluorescence analyses were performed as described in Figure 6a. Scale bar represents 50 μm. (b) The numbers of BrdU foci in these cells with or without MNU treatment were counted using the Image J software program with the BioVoxxel speckle inspector plug-in and plotted in a boxplot. * $p < 0.01$ (Student's *t*-test).

FIGURE 8 A model of the FAN1 function in the MMR-dependent apoptosis induced by O^6-methylguanine. The details are described in the text.

Figure 1 Rikitake *et al.*

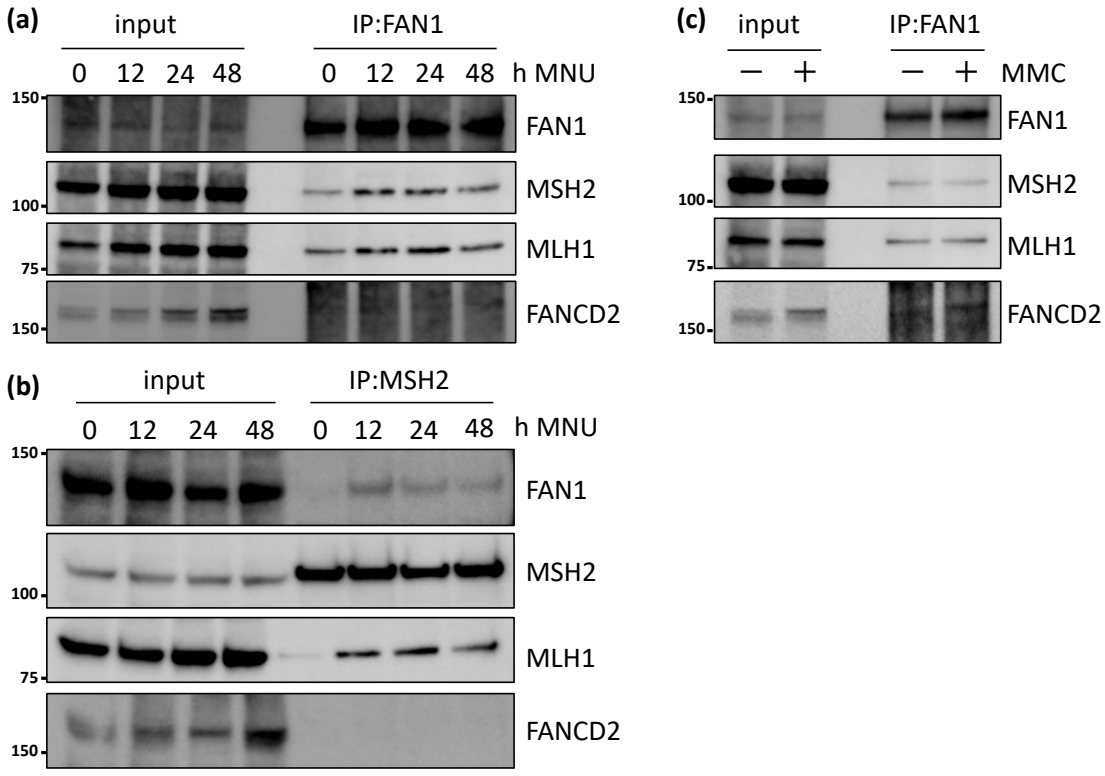

Figure 2 Rikitake *et al.*

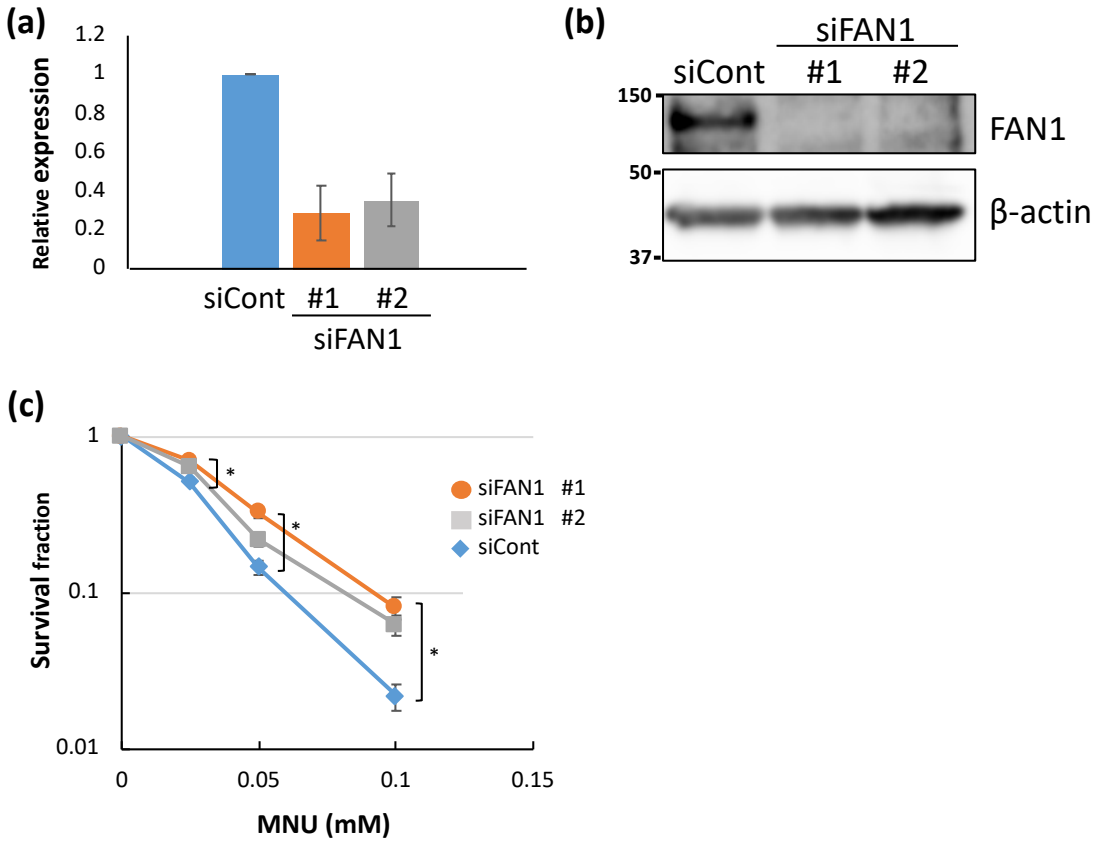

Figure 3 Rikitake *et al.*

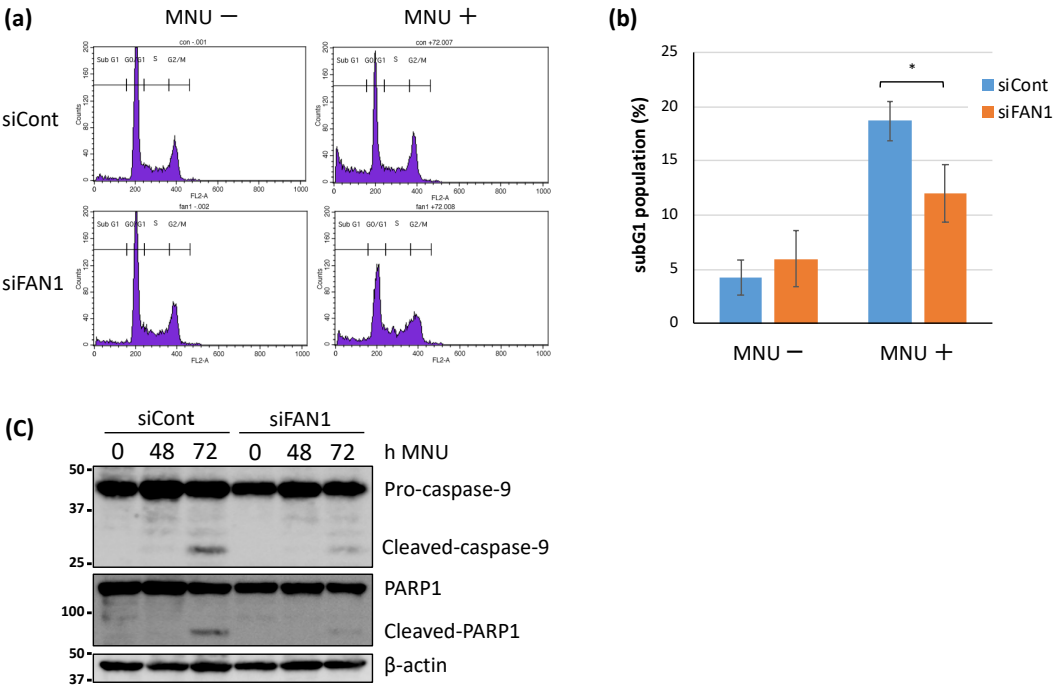

Figure 4 Rikitake *et al.*

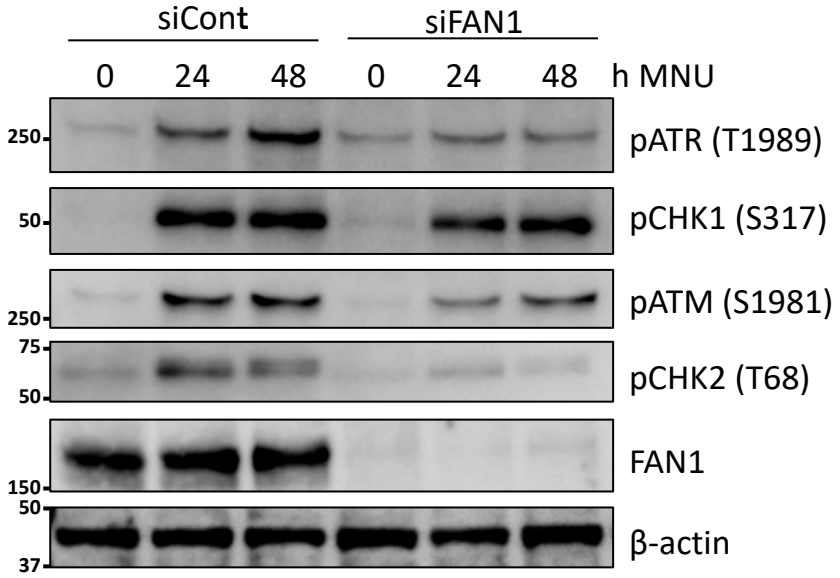

Figure 5 Rikitake *et al.*

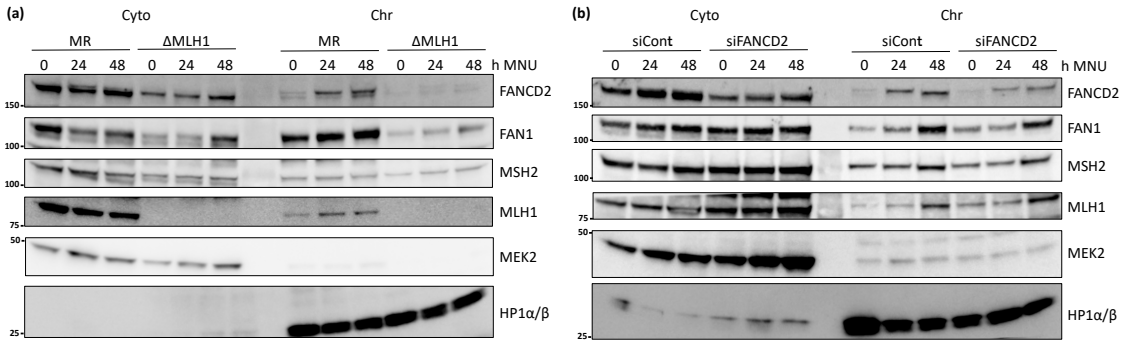

Figure 6 Rikitake *et al.*

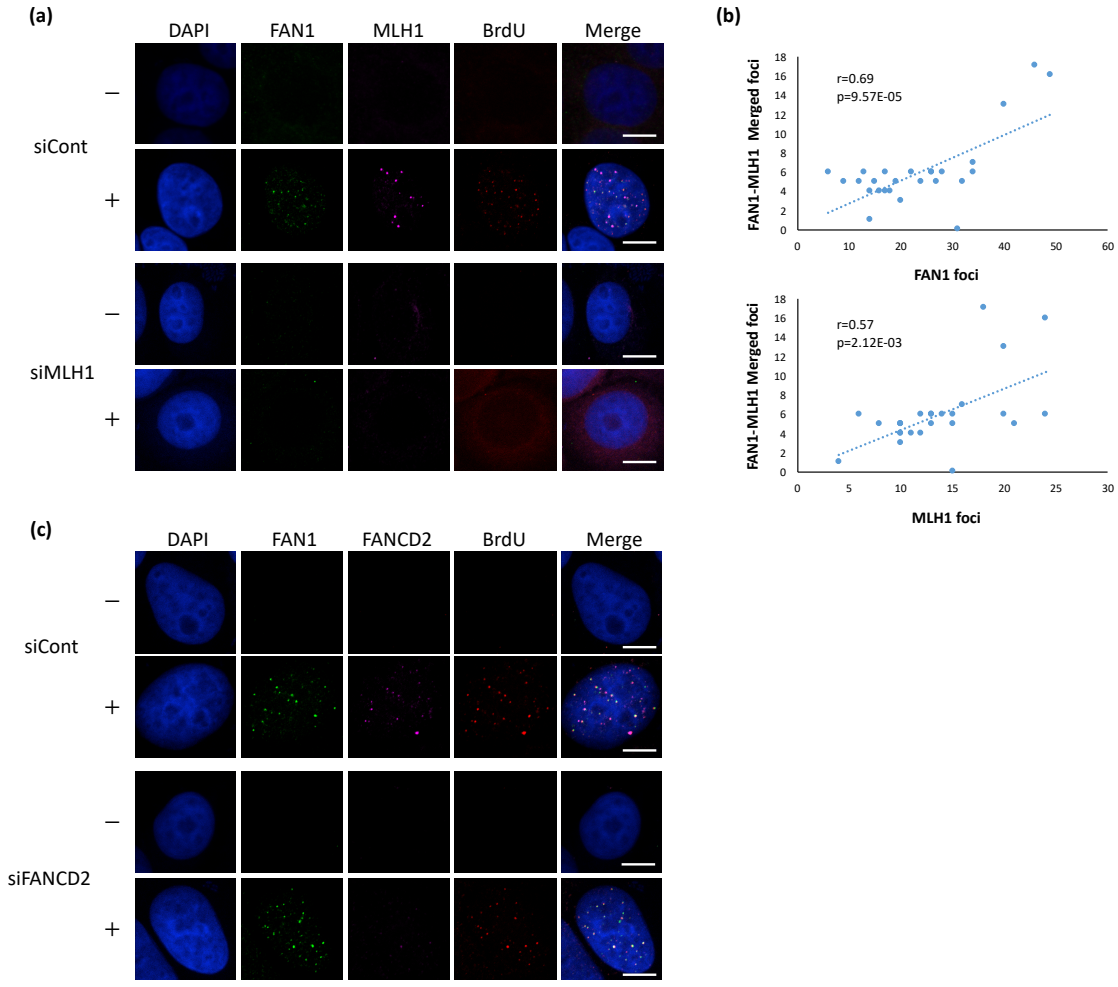

Figure 7 Rikitake *et al.*

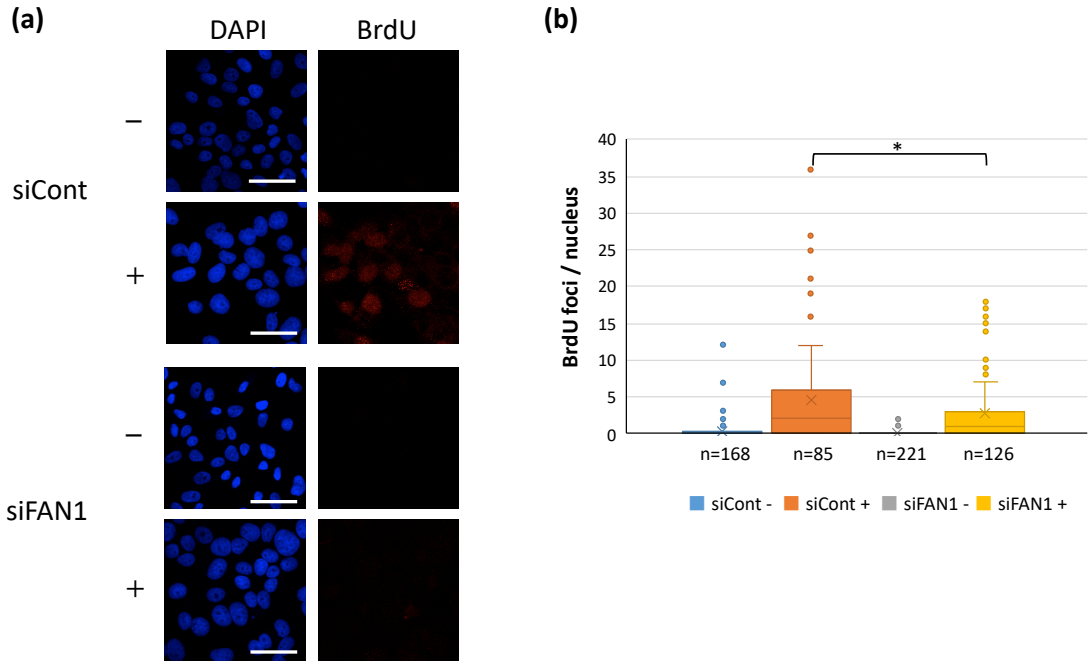

Figure 8 Rikitake *et al.*

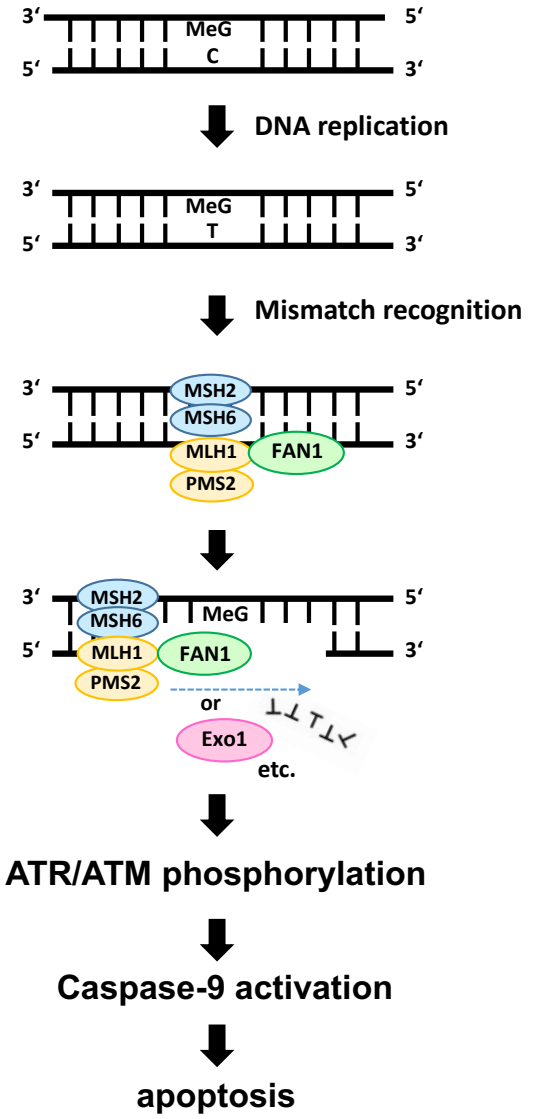

Supporting Information

MLH1-mediated recruitment of FAN1 to chromatin for the induction of apoptosis triggered by O^6-methylguanine

Mihoko Rikitake[1,2], Ryosuke Fujikane[1,3], Yuko Obayashi[1,4], Kyoko Oka[2], Masao Ozaki[2], and Masumi Hidaka[1,3,*]

From the [1]Department of Physiological Science and Molecular Biology, Fukuoka Dental College, Fukuoka, 819-0193, Japan, [2]Department of Oral Growth and Development, Fukuoka Dental College, Fukuoka, 819-0193, Japan, [3]Oral Medicine Research Center, Fukuoka Dental College, Fukuoka, 819-0193, Japan, [4]Department of Oral and Maxillofacial Surgery, Fukuoka Dental College, Fukuoka, 819-0193, Japan

A short title: Role of FAN1 in MMR-dependent apoptosis

KEYWORDS: apoptosis, FANCD2 and FANCI-associated nuclease 1 (FAN1), O^6-methylguanine, mismatch repair (MMR), MLH1

To whom correspondence should be addressed; Masumi Hidaka: Department of Physiological Science and Molecular Biology, Fukuoka Dental College, 2-15-1, Tamura, Sawara-ku, Fukuoka, 819-0193, Japan; E-mail: hidaka@college.fdcnet.ac.jp; Tel.: +81-92-801-0411.

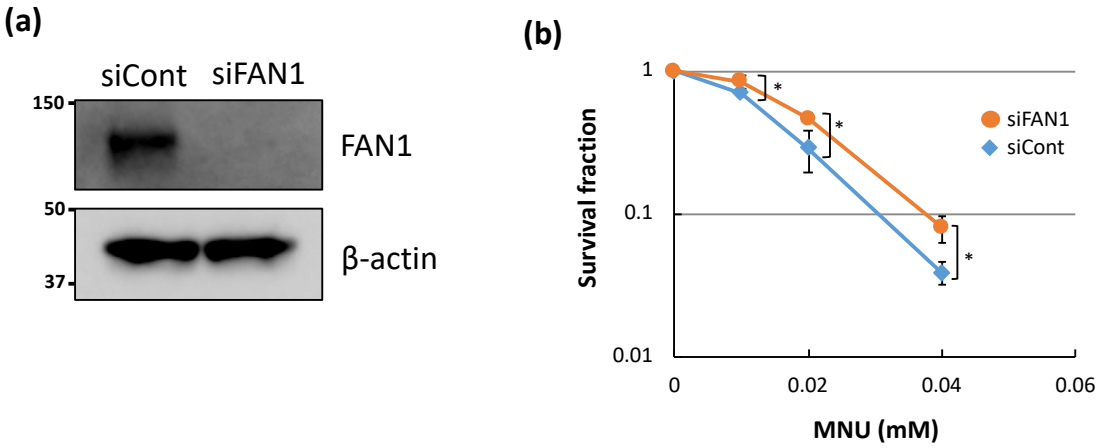

Figure S1 The sensitivity of *FAN1*-knockdown U2OS-derived cells to MNU. U2OSΔM cells were transfected with siRNA targeting to the *FAN1* gene. (a) The FAN1 protein levels at three days after siRNA-transfection were analyzed by immunoblotting. β-actin was the loading control. (b) The survival fraction of siRNA-transfected cells after MNU treatment. The cells were treated with various concentrations of MNU and the number of colonies formed at 12 days after the treatment was counted. The mean values of survival fraction obtained from three independent experiments is shown with the S.E. * $p < 0.05$ (Student's *t*-test).

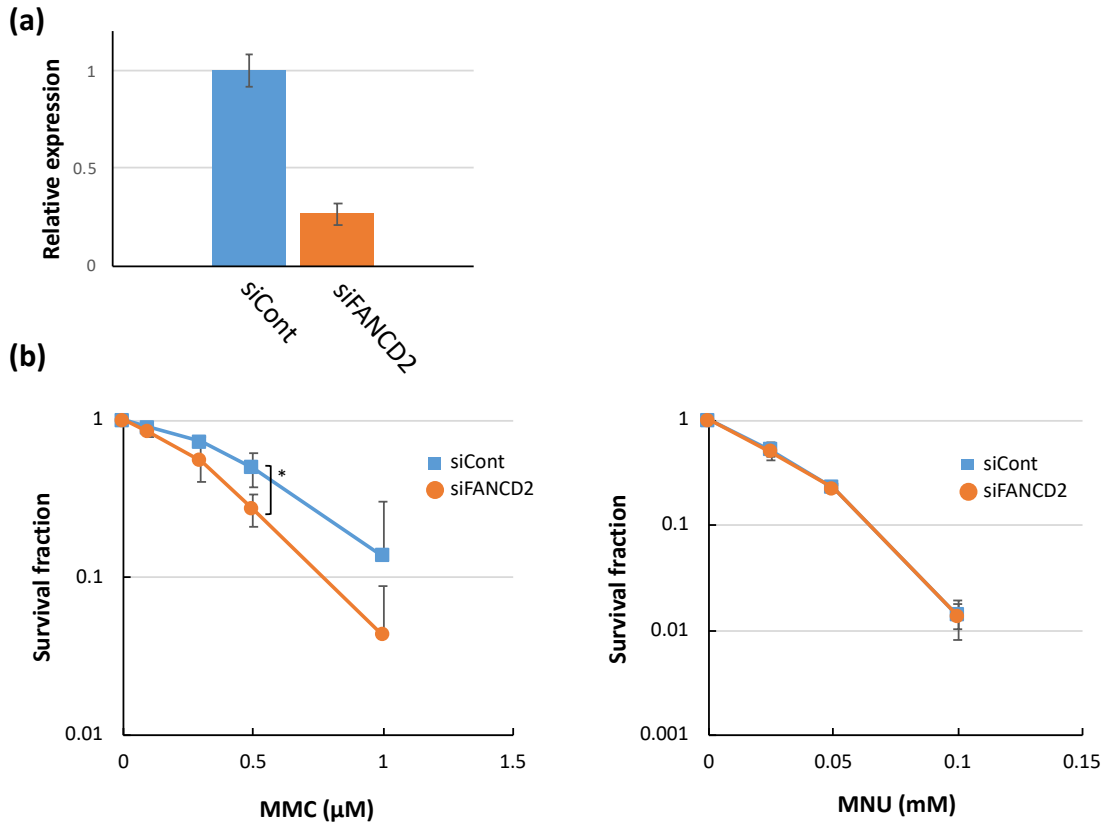

Figure S2 The sensitivity of *FANCD2*-knockdown cells to the treatment with MMC or MNU. (a) At 2 days after siRNA-transfection, the levels of mRNA of *FANCD2* were analyzed by quantitative PCR. The mean values of relative *FANCD2*-expression levels in comparison to control were obtained from three independent experiments and are shown with the S.E. (b) The survival fraction of siRNA-transfected cells after the administration of DNA damaging agents. The cells were treated with various concentrations of MMC (left) or MNU (right) and the number of colonies formed at 10 days after the treatment was counted. The mean values of survival fraction obtained from three independent experiments are shown with the S.E. * $p < 0.05$ (Student's *t*-test).

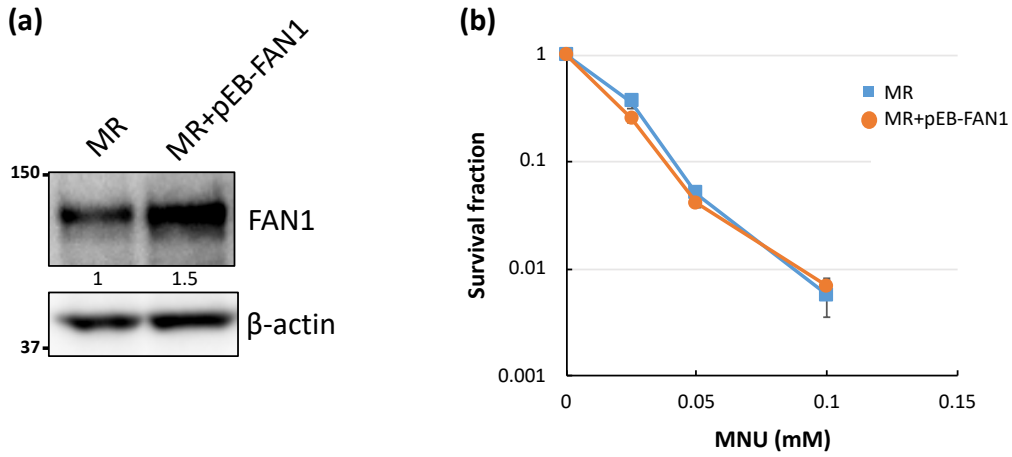

Figure S3 The sensitivity of FAN1 overexpressing cells to the treatment with MNU. (a) The level of total FAN1 protein in FAN1 overexpressing cells (MR+pEB-FAN1) was analyzed by an immunoblotting. β-actin was the loading control. The relative expression level of FAN1 protein normalized by β-actin were indicated below the panel. (b) The survival fraction of MR+pEB-FAN1 cells after MNU treatment. The cells were treated with various concentrations of MNU and the number of colonies formed at 10 days after the treatment was counted. The mean values of survival fraction obtained from three independent experiments are shown with the S.E.

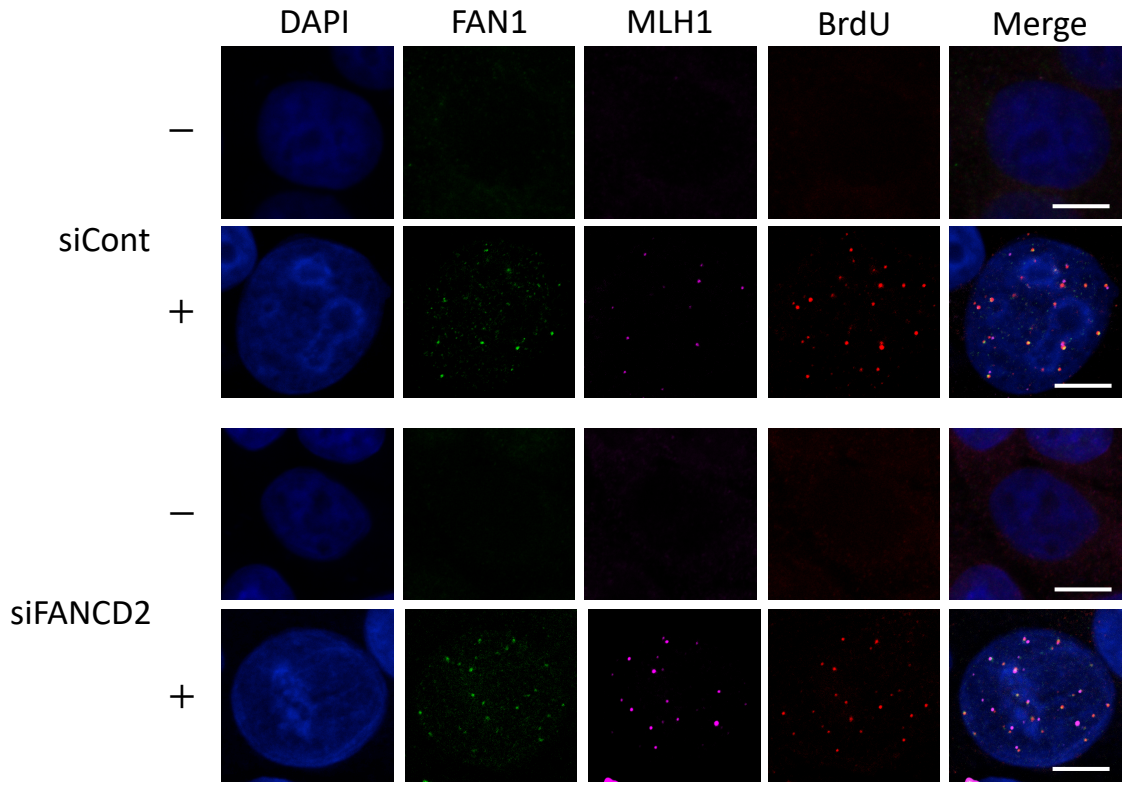

Figure S4 FAN1 forms nuclear foci with MLH1 and BrdU in a FANCD2-independent manner. Cells overexpressing FAN1 were transfected with siFANCD2 or siCont. Two days later, the cells were treated with 25 μM MNU or left untreated, and incubated for 48 h. The cells were permeabilized with 0.1% Triton X-100 and fixed with 4% paraformaldehyde, then immunofluorescence analyses were performed using the indicated antibodies. The nuclei were stained with DAPI. Scale bar represents 10 μm.

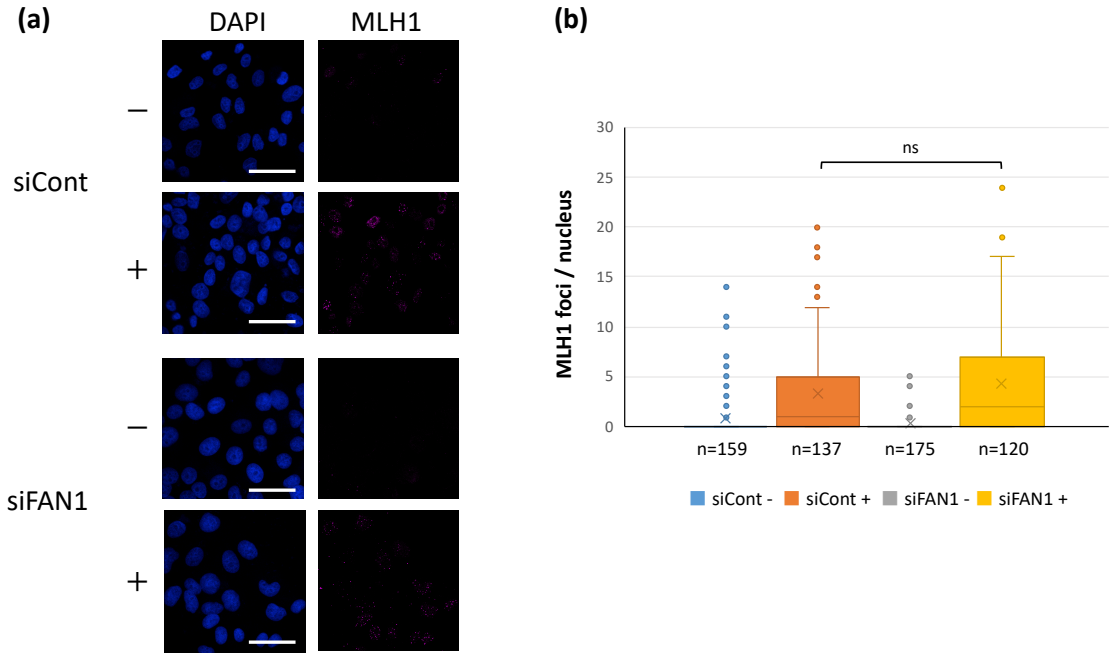

Figure S5 MLH1 forms nuclear foci in a FAN1-independent manner after MNU treatment. (a) HeLa MR cells transfected with siFAN1 or siCont were treated with 25 μM MNU or left untreated, and incubated for 48 h. Immunofluorescence analyses were performed as described in Figure 6a. Scale bar represents 50 μm. (b) The numbers of MLH1 foci in these cells with or without MNU treatment were counted using the Image J software program with the BioVoxxel speckle inspector plug-in and plotted in a boxplot. ns, not significantly different in Student's *t*-test).

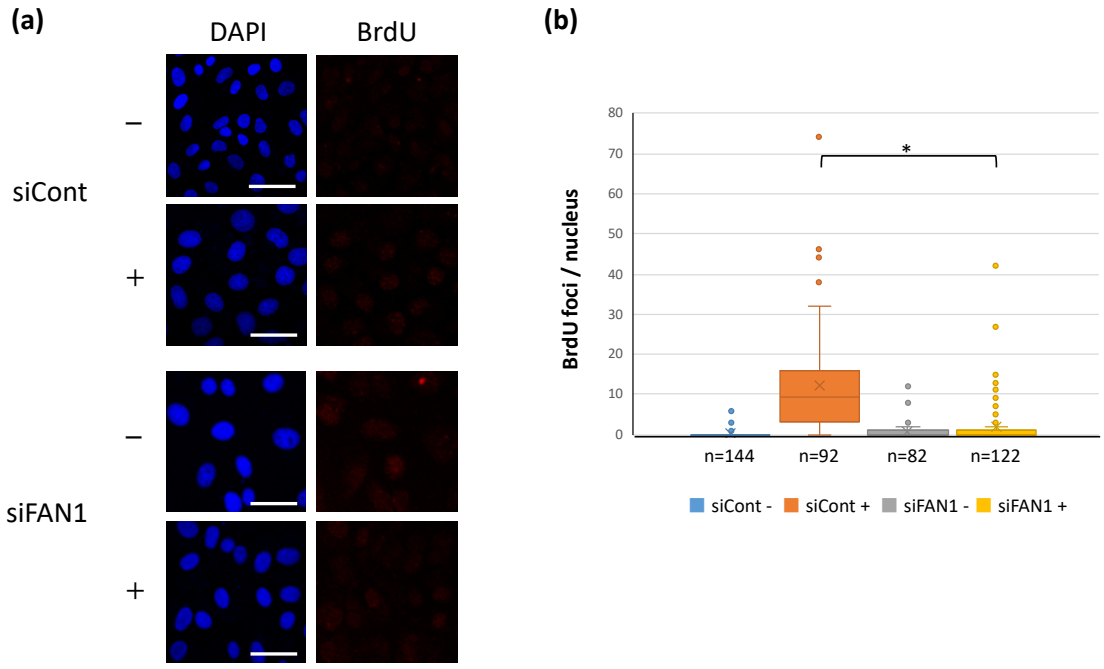

FIGURE S6 The effects of *FAN1*-knockdown on the formation of ssDNA in *MGMT*-knockout U2OS cells. (a) U2OSΔM cells transfected with siFAN1 or siCont were treated with 25 μM MNU or left untreated, and incubated for 48 h. Immunofluorescence analyses were performed as described in Figure 6a. Scale bar represents 50 μm. (b) The numbers of BrdU foci in these cells with or without MNU treatment were counted using the Image J software program with the BioVoxxel speckle inspector plug-in and plotted in a boxplot. * $p < 0.01$ (Student's *t*-test).